ehp ENVIRONMENTAL HEALTH PERSPECTIVES
http://www.ehponline.org

Effects of Laser Printer–Emitted Engineered Nanoparticles on Cytotoxicity, Chemokine Expression, Reactive Oxygen Species, DNA Methylation, and DNA Damage: A Comprehensive *in Vitro* Analysis in Human Small Airway Epithelial Cells, Macrophages, and Lymphoblasts

Sandra V. Pirela, Isabelle R. Miousse, Xiaoyan Lu, Vincent Castranova, Treye Thomas, Yong Qian, Dhimiter Bello, Lester Kobzik, Igor Koturbash, and Philip Demokritou

http://dx.doi.org/10.1289/ehp.1409582

Received: 10 December 2014
Accepted: 12 June 2015
Advance Publication: 16 June 2015

Environ Health Perspect DOI: 10.1289/ehp.1409582
Advance Publication: Not Copyedited

Effects of Laser Printer–Emitted Engineered Nanoparticles on Cytotoxicity, Chemokine Expression, Reactive Oxygen Species, DNA Methylation, and DNA Damage: A Comprehensive *in Vitro* Analysis in Human Small Airway Epithelial Cells, Macrophages, and Lymphoblasts

Sandra V. Pirela[1], Isabelle R. Miousse[2], Xiaoyan Lu[1], Vincent Castranova[3], Treye Thomas[4], Yong Qian[5], Dhimiter Bello[1,6], Lester Kobzik[1], Igor Koturbash[2], and Philip Demokritou[1]

[1]Department of Environmental Health, Center for Nanotechnology and Nanotoxicology, Harvard T.H. Chan School of Public Health, Harvard University, Boston, Massachusetts, USA; [2]Department of Environmental and Occupational Health, University of Arkansas for Medical Sciences, Little Rock, Arkansas, USA; [3]Department of Pharmaceutical Sciences, West Virginia University, Morgantown, West Virginia, USA; [4]Office of Hazard Identification and Reduction, U.S. Consumer Product Safety Commission, Rockville, Maryland, USA; [5]Pathology and Physiology Research Branch, Health Effects Laboratory Division, National Institute for Occupational Safety and Health, Morgantown, West Virginia, USA; [6]Department of Work Environment, University of Massachusetts, Lowell, Massachusetts, USA

Address correspondence to Philip Demokritou, Department of Environmental Health, Harvard T.H. Chan School of Public Health, Harvard University, 665 Huntington Avenue, Room 1310B, Boston, Massachusetts 02115 USA. (617) 432-3481. E-mail: pdemokri@hsph.harvard.edu

Running title: Toxicity of nanoparticles from laser printers

Acknowledgments: The authors acknowledge funding for this study from NIEHS Center Grant ES-000002, NIOSH and CPSC (Grant # 212-2012-M-51174), NIH HL007118, UAMS/NIH Clinical and Translational Science Award UL1TR000039 and KL2TR000063, and the Arkansas Biosciences Institute, major research component of the Arkansas Tobacco Settlement Proceeds Act of 2000.

Competing financial interests: The authors declare they have no competing financial interests.

Abstract

Background: Engineered nanomaterials (ENMs) incorporated into toner formulations of printing equipment become airborne during their consumer use. Although information on the complex physicochemical and toxicological properties of both toner powders and printer-emitted particles (PEPs) continues to grow, most toxicological studies have primarily used raw toner powders rather than the actual PEPs, which are not representative of current exposures experienced at the consumer level during printing.

Objectives: To assess the biological responses of a panel of human cell lines to PEPs.

Methods: Three physiologically relevant cell lines—small airway epithelial cells (SAEC), macrophages (THP-1 cells) and lymphoblasts (TK6 cells)—were exposed to PEPs at a wide range of doses (0.5-100 μg/mL) that correspond to human inhalation exposure durations at the consumer level of ~ 8 hours and higher. Following treatment, toxicological parameters reflecting distinct mechanisms were evaluated.

Results: PEPs caused significant membrane integrity damage, an increase in reactive oxygen species (ROS) production as well as a rise in pro-inflammatory cytokine release in different cell lines at doses relevant to exposure durations from 7.8 to 1500 hours. Furthermore, there were differences in methylation patterns that although statistically insignificant, demonstrate the potential PEPs can have on the overall epigenome following exposure.

Conclusions: The *in vitro* findings here suggest that laser printer-emitted engineered nanoparticles may be deleterious to lung cells, and provide preliminary evidence of epigenetic modifications that might translate to pulmonary disorders.

Introduction

The recent incorporation of engineered nanomaterials (ENMs) into toner formulations has possible health implications based on consumer exposure to released particulate matter (PM) from laser-based printing equipment. Laser printers are widely used in office and home environments with an exponential increase of market sales in recent years (IDC 2014). Recent studies have shown that emissions from this growing technology comprise a variety of pollutants including PM, semi-volatile organic compounds (sVOCs) and other gaseous pollutants (He et al. 2007; Morawska et al. 2009; Wang et al. 2012).

Recently, our group developed a lab based Printer Exposure Generation System (PEGS) that allows generation and sampling of airborne printer-emitted particles (PEPs) for subsequent physicochemical, morphological and toxicological analysis (Pirela et al. 2014a). This platform was used to evaluate emission profiles from 11 laser printers currently on the market. The study showed the particle number concentration of PEPs varied across different printers/manufacturers reaching up to 1.3 million particles/cm^3 with diameters <200 nm (Pirela et al. 2014a). The detailed assessment of both toners and PEPs confirmed presence of nanoscale materials in the airborne state and a complex chemistry, which included elemental/organic carbon and inorganic compounds (*e.g.*, metals, metal oxides). Thus, confirming toners are nano-enabled products (NEPs) (Pirela et al. 2014b).

Both *in vitro* and *in vivo* toxicological assays may help characterize the effects of laser printer emissions and toners on the respiratory system. However, the results to date are contradictory. Notably, the toxicity of PEPs remains poorly characterized primarily because most studies used toner powders rather than PEPs. For example, Gminski et al. (2011) reported toner powders exhibited genotoxic potential on epithelial lung cells. Additionally, similar *in vitro*

assays using an air/liquid interphase system, showed significant cyto- and genotoxicity (Tang et al. 2012). In contrast, exposure of alveolar macrophages to toner powder revealed no effect using cell magnetometry analysis (Furukawa et al. 2002). An even smaller number of *in vivo* toxicological studies have been evaluated effects of PEPs exposures. Bai et al. (2010) reported that mice exposed to printer toner particles showed significant pulmonary inflammation, damage to the epithelial-capillary barrier and enhanced cell permeability. Comparable inflammatory and fibrotic responses were also observed in rats exposed to toner powders (Morimoto et al. 2013).

Concerns continue to be raised in terms of possible epigenetic effects associated with PEPs inhalation exposures. In general, the ability of ENMs to affect the cellular epigenome remains largely unexplored. One important epigenetic mechanism, DNA methylation, can regulate proper expression of genetic information in a sex-, tissue-, and cell type-dependent manner (Jones 2012). Additionally, DNA methylation plays a central role in regulating the expression of transposable elements (TEs) that comprise a large part of the eukaryote genome (Smith et al. 2012). TEs are essential regulators of stability and proper function of the genome, including expression of genetic information and chromatin structure. Numerous studies indicate that exposure to various environmental stressors, including PM, may compromise the methylome and TEs (Baccarelli et al. 2009; Madrigano et al. 2011). An *in vitro* study by Gong et al. (2010) concluded that short-term exposure of human keratinocytes to nanomaterials might result in alterations in both global DNA methylation patterns and the DNA methylation machinery. However, the epigenetic effects of ENMs contained in PEPs remain largely unknown, and, to our knowledge, epigenetic effects as a result of exposure to PEPs using *in vitro* systems have yet to be characterized.

In the present *in vitro* toxicological study, the biological responses due to exposure to PEPs on physiologically relevant cells: human small airway epithelial cells (SAEC), macrophages (THP-1 cells) and lymphoblasts (TK6 cells) were evaluated using a wide range of exposure doses. Several endpoints (*e.g.,* cell membrane integrity, ROS production, DNA methylation) important for the understanding of mechanisms of toxicity were assessed in this study taking into consideration *in vitro* and *in vivo* dosimetry. Such thorough physicochemical, morphological and cellular toxicological characterization studies based on the "real world" exposure conditions adds to the body of scientific evidence required to understand and quantify the exposure risk to PEPs from the use of printing equipment. More importantly, the proposed methodology can be used to assess risks associated to ENMs released across life cycle of any other nano-enabled product.

Materials and Methods

Generation and collection of size-fractionated PEPs

The PEPs were generated using the recently developed PEGS as described in our recent publication (Pirela et al. 2014a). In summary, the PEGS was used to generate, collect and sample size-fractionated PEPs from a high emitting printer (referred to as Printer B1 in companion papers) emitting up to 1.26 million particles/cm^3 (Pirela et al. 2014a).

Post sampling physicochemical and morphological characterization of PEPs

Detailed chemical and morphological characterization of the PEPs and toner from the test printer, as well as the paper utilized in this study, are presented in detail in a recently published companion publication (Pirela et al. 2014b). In summary, toner powder and PEPs share a similar chemical fingerprint, respectively containing 62 and 97% organic, 10 and 0.5% elemental

carbon, ~3% metal/metal oxides (*e.g.*, aluminum, titanium) and ~25% of other elements (*e.g.*, phosphorus, sulfur) (Pirela et al. 2014b).

Extraction of size fractionated PEPs, preparation and characterization of particle liquid suspensions for cellular studies

After sampling size-fractionated PEPs, the particles were extracted from collection filter media using an aqueous suspension methodology (Demokritou et al. 2002; Pirela et al. 2014b). Subsequently, particle dispersions in culture media were prepared using a protocol developed by the authors (Cohen et al. 2013), in which the particle critical delivered sonication energy (DSE_{cr}), hydrodynamic diameter (d_H), formed agglomerate size distribution, polydispersity index (PdI), zeta potential (ζ), specific conductance (σ), pH, colloidal stability and effective density of formed agglomerates (DeLoid et al. 2014) are measured. PEPs dispersion values are given in Table 1. Prior to use in experiments, particle suspensions were prepared with sterile deionized water (DI H_2O), sonicating at DSE_{cr} and diluting to desired final test concentrations in the respective media. It is worth noting that the effective density of the formed agglomerates, which plays an important role in the settling and dosimetry *in vitro*, was measured using the recently developed Volumetric Centrifugation Method (VCM) (DeLoid et al. 2014).

***In vitro* and *in vivo* dosimetric considerations**

To express *in vivo* and *in vitro* doses on the same scale, the dosimetric approach recently developed by the authors was followed (Demokritou et al. 2013b). In summary, the Multiple-Path Particle Dosimetry model (MPPD2) (Anjilvel and Asgharian 1995) is used to calculate the deposition mass flux in the human lung ($\mu g/m^2 \bullet min$) and the deposited PEPs mass per area ($\mu g/m^2$) following an inhalation exposure to PEPs for a determined amount of time.

Supplemental Material, Table S1 summarizes the parameters used for the MPPD2 simulations, which includes both the airborne nanoparticle size distribution values (count median diameter, geometric standard deviation, particle mass concentration) and the human breathing parameters of a resting individual (tidal volume, breathing frequency, inspiratory fraction, pause fraction, functional residual capacity, head volume, breathing route). The calculated mass per area deposited in the lung obtained from the model is the equivalent mass per area ($\mu g/m^2$) that needs to be delivered to cells in the *in vitro* experiment (mass deposited *in vitro*).

Subsequently, because of the particokinetics of the PEPs-media suspension that define their settling rate, the delivered to cell *in vitro* mass is not necessarily equal to the administered *in vitro* mass. Therefore, the fraction of administered particle mass that is deposited on the cells as a function of *in vitro* exposure time (f_D) needs to be calculated in order to match the *in vivo* lung deposited dose estimated by the MPPD2 model. The f_D as a function of *in vitro* exposure time is calculated using the hybrid Volumetric Centrifugation Method-*In Vivo* Sedimentation, Diffusion and Dosimetry (VCM-ISDD) methodology (Cohen et al. 2014b; DeLoid et al. 2014; Pal et al. 2014), recently developed by the authors. The mean media-formed agglomerate d_H and the VCM-measured effective density of formed agglomerates (DeLoid et al. 2014) were used as input to the VCM-ISDD fate and transport numerical model in order to estimate the f_D as a function of time. For more details, please refer to Supplemental Material, Part A: Dosimetric considerations for *in vitro* testing – Example of calculations.

Source and characterization of comparative particles (controls) used in the study

The gas metal arc-mild steel welding fumes (MS-WF) were used as comparative material for the study and were provided by Dr. J. Antonini from the National Institute for Occupational Health (NIOSH). The sample was generated as described in Antonini et al. (1999), and has a

count mean diameter of 1.22 μm and has been shown to induce toxicity in the lungs of rodents (Antonini et al. 2012; Sriram et al. 2012; Zeidler-Erdely et al. 2011). Its Brunauer-Emmett-Teller (BET, Quantachrome) specific surface area was found to be 48.2 m^2/g and its equivalent primary particle diameter was estimated to be 23.8 nm. The amorphous silicon dioxide (SiO_2) was generated in-house using the Harvard Versatile Engineered Nanomaterial Generation System (VENGES) as previously described (Demokritou et al. 2010; Sotiriou et al. 2012) and had a BET measured primary particle diameter of 14.7 nm. Both materials were used as comparative materials due to the extensive toxicological data in the current body of literature.

Cell culture

The human monocytic immortalized cells (THP-1, American Type Culture Collection) were cultured in Roswell Park Memorial Institute Medium (RPMI) 1640 supplemented with 10% fetal bovine serum (FBS). The small airway epithelial cells (SAEC) were obtained from NIOSH and cultured in serum-free small airway epithelial cell growth medium (SAGM) with the addition of multiple supplemental growth factors provided by the manufacturer (Lonza, Inc.). The TK6 human lymphoblastoid cell lines were maintained in RPMI 1640 with L-glutamine supplemented with 10% horse serum (HS). It is worth noting that the TK6 lymphoblast cell line used here may not be directly physiologically relevant to lung toxicology. However, this cell line has been used historically for genotoxicity evaluations due to its increased sensitivity for DNA damage assessments, in particular when performing the comet assay (Bajpayee et al. 2013; Kimura et al. 2013). Here, TK6 cells were used to rank PEPs in terms of DNA damage potential based on this past record of utility. All media were supplemented with 1% penicillin-streptomycin. Generic cell culture protocol consisted of growing cells in an incubator (37°C/5%

CO_2) in 25- or 150-cm^2 flasks, replacing media every 2–3 days and passaging before confluence. Before exposure, THP-1 cells were differentiated into macrophages (Daigneault et al. 2010).

Cellular assays

Various cellular assays were used to assess biological mechanisms. All experiments were performed in triplicate. In more detail:

Cellular membrane integrity. Following exposure to the test particles, cells were evaluated for viability using the CytoTox-One Homogenous Membrane Integrity Assay (Promega). This assay estimated the number of non-viable cells present after exposure by measuring the activity of lactate dehydrogenase (LDH) leaked from the cell.

ROS production. At 23.5 hours of particle exposure, 5-μM dihydroethidium (DHE) was added to each treatment well and incubated for 30 minutes. Fluorescent measurements were taken immediately using a fluorescence microplate reader (Molecular Devices) at an excitation of 518 nm and emission detection of 605 nm. Hydrogen peroxide was used as a positive control in this assay and while these measurements were not shown in the figure, they were used in the calculations to normalize the data.

Autofluorescence of ENMs pertaining to both the cellular membrane integrity and ROS assays. The autofluorescence of ENMs and media can cause interference with fluoroscopic bioassays (Doak et al. 2009; Holder et al. 2012; Monteiro-Riviere et al. 2009) and control experiments for both particle- and media-only need to be included in the measurement to consider particle/media interference. We have performed such experiments in this study in order to estimate potential nanoparticle interference/absorption in the LDH and ROS assay and measured the fluorescence intensity of the particles suspended in media. The intensity was found

minimal and similar to that of the media-alone control for both bioassays and this was included in the calculations (results not shown).

DNA damage. To assess the potential genotoxic properties of PEPs, the high throughput Nano-CometChip assay, recently developed by our group, was used to measure DNA double stranded breaks on TK6 cells following a four-hour exposure to particles as described in Watson et al. (2014).

Epigenetic analysis. A number of assays were performed to evaluate DNA methylation patterns on SAEC exposed to PEPs (0.5 and 30 μg/mL administered doses) for 24 hours. In more detail:

Methylation of transposable elements: RNA and DNA were extracted simultaneously from SAEC using the AllPrep Mini Kit (Qiagen) according to the manufacturer's protocol. Analysis of methylation and expression of transposable elements was performed as reported earlier (Lu et al. 2015). Briefly, 500 ng of gDNA was treated with 0.5 U of SmaI, HpaII, HhaI, AciI, and BstUI enzymes in 1X CutSmart buffer. The resulting digested DNA was analyzed by quantitative real-time PCR (qRT-PCR) using 2 ng per reaction and SYBR Select chemistry (Life Technologies). Primers are listed in Supplemental Material, Table S2.

Expression of transposable elements: cDNA was synthesized from 1 μg RNA using the High-Capacity Reverse Transcription Kit (Life Technologies). qRT-PCR was performed using 10 ng of cDNA per reaction and SYBR Select chemistry (Life Technologies) on a ViiA 7 instrument (Life Technologies). Primers are listed in Supplemental Material, Table S2. Expression was calculated using the ΔΔCT method and normalized to the internal control *Gapdh*.

LINE-1 copy numbers analysis: LINE-1 copy number was assessed as previously described (Miousse et al. 2014). Briefly, LINE-1 ORF1 was amplified by qRT PCR from 10 ng of gDNA. The FAM/ZEN-conjugated primers with the probe sequence (Integrated DNA Technologies) are shown in Supplemental Material, Table S3. Relative abundance of the target in gDNA was normalized to 5S ribosomal DNA using the ΔΔCt method.

Cytokine and chemokine analysis

Supernates from treated SAEC were assayed by Eve Technologies Corporation using a Human Primary Cytokine Array/Chemokine Array 41-Plex Panel (Millipore) according to the manufacturer's protocol.

Statistical analysis

Statistical analyses were performed using GraphPad Prism 6.0. Comparisons between all cellular parameters after exposure were evaluated using one-way analysis of variance and Tukey correction for multiple comparison statistical significance. A p value < 0.05 was considered significant. Experiments were conducted in triplicate.

Results

PEPs dispersion and characterization

Supplemental Material, Figure S1 shows the hydrodynamic diameters for both PEPs and MS-WF plotted as a function of Delivered Sonication Energy (DSE). It can be observed that as the DSE increases, the dynamic light scattering (DLS)-measured d_H decreases towards a marginal state of minimal agglomeration. The DSE_{cr} for PEPs ($PM_{0.1}$) was 514.29 J/mL. Similarly, MS-WF had a DSE_{cr} of 400 J/mL. The DSE_{cr} for SiO_2 was obtained from a previous publication and was found to be 242 J/mL (Cohen et al. 2013).

Table 1 summarizes the particle colloidal properties in both DI H_2O and different types of biological media used, including the DLS-measured hydrodynamic diameter (d_H), zeta potential (ζ), polydispersity index (PdI), specific conductance (σ) and pH. The suspension of PEPs ($PM_{0.1}$) demonstrated a lower d_H in DI H_2O when compared to that in cellular media. PEPs ($PM_{0.1}$) had a d_H of 178.3 nm, which increased to >200 nm when dispersed in media. This is in agreement with literature (Cohen et al. 2013) as it is anticipated that presence of proteins will induce formation of a thicker protein corona on particle agglomerates. MS-WF in suspension had a d_H of 2197 nm in DI H_2O, which decreased when dispersed in media to values ranging from 1502-1878 nm. Lastly, the d_H of silica was 142.5 nm in DI H_2O and 114.6-207.7 nm in media. Observed values of zeta potential were strongly negative for the PEPs in DI H_2O (-20.6 mV) and became less negative in various media. MS-WF and SiO_2 had positive zeta potentials in DI H_2O and media. In addition to d_H measurements, colloidal size stability of particle suspensions was subsequently evaluated for 24 hours. It was observed that d_H of PEPs, SiO_2 and MS-WF suspended in SAGM remained fairly stable for up to 24 hours.

Additionally, the VCM-measured effective density of PEPs ranged from 1.19-2.39 g/cm^3 in different cellular media used, while those of the comparator materials used in the study were approximately 1.2 g/cm^3 for SiO_2 and 1.37-1.56 g/cm^3 for MS-WF (Table 1). It is worth noting that effective density and size of formed agglomerates are important determinants of fate and transport in the *in vitro* system and define settling rates and dosimetry *in vitro* (DeLoid et al. 2014 Cohen et al. 2013, Pal et al. 2015).

Dosimetric considerations for *in vitro* testing

The delivered to cell dose at a given exposure time point may not always be the same as the dose administered (Cohen et al. 2013). Using the recently developed Harvard *in vitro* dosimetry methodology (Cohen et al. 2014b), the fraction of the administered particles that deposited on the cells located at the bottom of the treatment well as a function of time was calculated and presented in Supplemental Material, Figure S2. As expected, some of the materials used in the study settled faster than other. For instance, it will take less than two hours for all of the administered MS-WF mass, suspended in either RPMI/10%FBS or SAGM, to deposit on the cells. For silica, only approximately 35% and 100% of the administered dose will actually reach the bottom of the well in the 24-hour exposure when suspended in RPMI/10%FBS and SAGM, respectively. Interestingly, for the same exposure duration, 100% and 51.8% of the administered dose of PEPs will be deposited to the cells when suspended in SAGM and RPMI/10%FBS, respectively. This translated to a respective f_D of 1.00 and 0.518 for PEPs. The estimated deposited mass of administered particle mass for all PEPs doses and exposure times is summarized in Table 2 (see Supplemental Material, Table S4 for estimated deposited mass for SiO_2 and MS-WF).

Additionally, in order to bring *in vitro* and *in vivo* doses to the same scale, the deposition mass flux of PEPs in a human lung was determined to be 1.732 $\mu g/m^2 \bullet min$ using the MPPD2 model. This calculated mass flux was then used to back calculate the inhalation exposure durations to PEPs corresponding to the range of administered doses used in this study (summarized in Table 2). Based on dosimetric calculations for THP-1 monocytes, the lowest *in vitro* PEPs administered dose used in this study is consistent with an inhalation exposure lasting for 7.8 hours of printing, whereas the higher administered dose (100 μg/mL) used would

correspond to hundreds of hours of exposure. The wide range of corresponding human exposures to laser printer emissions evaluated here, makes the doses relevant for individuals in both occupational and consumer settings. The majority of the inhaled PEPs would deposit in the respiratory bronchioles and distal alveoli (Supplemental Material, Figure S3). Approximately 31% of inhaled PEPs would deposit in the tracheobronchial region and 18.4% would be deposited in the head region. Although the selection of cell lines in this study reflects those located in the lower respiratory area, it should be noted that the upper airways are an equally interesting target.

Effects of PEPs on cell viability

Cellular membrane integrity of all three human cell lines studied was decreased following exposure to PEPs. Figure 1 illustrates results from the lactate dehydrogenase assay, showing percent cytotoxicity of each treatment at various administered doses. In particular, SAEC experienced >40% cell death after exposure to PEPs ($PM_{0.1}$, 100 μg/mL administered dose) when compared to untreated cells. Macrophages (THP-1 cells) exposed to PEPs ($PM_{0.1}$) exhibited a significant increase cell death in a dose-response manner, which was greater than MS-WF or SiO_2 treatment, where MS-WF is known to be cytotoxic (Antonini et al. 1999; Antonini et al. 2012; Zeidler-Erdely et al. 2011). Lastly, cytoxicity decreased with increasing exposure to PEPs ($PM_{0.1}$) in human lymphoblasts (TK6 cells), though differences among dose groups were not significant.

Effects of PEPs on ROS production

To evaluate the potential of PEPs to induce ROS production in epithelial cells (SAEC) and macrophages (THP-1 cells), two cell lines that are in direct contact with inhaled foreign

material, the levels of superoxide ions were measured. Figure 2 illustrates the results from the DHE fluorescence on each of the treatments at the various exposure doses showing contrasting responses in both cell lines. A clear dose-response relationship was observed in SAEC treated with PEPs. While MS-WF and SiO_2 also enhanced ROS production in SAEC, dose dependence was not observed. The level of ROS production with PEPs (100 μg/mL, administered dose) was similar to that with 100 μg/mL MS-WF or SiO_2 in SAEC. Macrophages (THP-1 cells) displayed elevated superoxide levels following exposure to PEPs (5 μg/mL, administered dose), while higher doses did not induce ROS production. Treatment with PEPs (5 μg/mL) was more potent in stimulating ROS release than SiO_2 or MS-WF at the same administered dose.

Effects of PEPs on inflammatory mediator secretion

Cytokine/chemokine release plays an important role in the regulation of an immune response towards pathogens or injury (Lacy and Stow 2011). In order to evaluate the effect of PEPs on such biological reactions, levels of a wide range of these mediators were measured in SAEC following a 24-hour exposure to PEPs (5 and 40 μg/mL, administered doses). Of 41 measured cytokines/chemokines, six of them, namely monocyte chemotactic protein (MCP)-1, macrophage inflammatory protein (MIP)-1b, platelet-derived growth factor (PDGF)-AA, interleukin (IL)-1RA, IL-6 and RANTES were significantly increased in SAEC exposed to PEPs ($PM_{0.1}$) (Figure 3). Levels of MCP-1, MIP-1b, RANTES, PDGF-AA and IL-6 were significantly higher after PEPs exposure (40 μg/mL, administered dose) than in the untreated cells. In addition, there was a significant difference in levels of MIP-1b and IL-6 in SAEC exposed to both doses of PEPs (5 and 40 μg/mL, administered dose). Exposure to PEPs (5 μg/mL,

administered dose) led to a significant rise in IL-1RA and PDGF-AA secretion when compared to untreated cells.

Effects of PEPs on genotoxicity in TK6 lymphoblasts

To evaluate the genotoxicity potential of PEPs, a DNA damage assessment was performed on human lymphoblasts (TK6 cells), which are genetically sensitive to chemical exposures (Ayres et al. 2006; Kimura et al.). Results from the Nano-CometChip assay show PEPs did not inflict significant DNA damage on the lymphoblasts (Supplemental Material, Figure S4). Likewise, neither of the comparative testing particles (SiO_2, MS-WF) produced induction of single-stranded DNA damage when compared to untreated cells.

Effects of PEPs on global and TEs-associated DNA methylation

L1 repetitive element comprises ~17% of the human genome, is heavily methylated, and therefore its methylation status is generally accepted as a surrogate biomarker for global DNA methylation (Miousse et al. 2015). Therefore, to investigate whether or not short-term exposure to PEPs can affect the global DNA methylation, methylation patterns of both L1 open reading frames (ORF1, ORF2) were evaluated. A loss of DNA methylation is observed in ORF1 and ORF2, respectively, although not statistically significant (*p* value 0.09, in both cases) after exposure to PEPs (0.5 μg/mL, administered dose) compared to untreated cells. No significant changes in DNA methylation were detected after exposure to an administered dose of 30 μg/mL of PEPs (Figure 4A).

Alu elements are another group of TEs that are highly abundant in the human genome (comprising ~10%), correspond to SINE elements in mice and can be affected by exogenous stressors (Rudin and Thompson 2001). Thus, we addressed whether the methylation of *Alu*

elements is also affected by PEPs by examining the AluYb11 subfamily belonging to SINE1/7SL family of evolutionary-recent *Alu* elements. Based on comparisons with untreated cells, treatment with 0.5 μg/mL (administered dose) of PEPs led to ~70% decrease in *Alu* methylation, although insignificant, while exposure to 30 μg/mL (administered dose) PEPs did not affect methylation of *Alu* (Figure 4A).

Effects of PEPS on TEs expression

TEs methylation is a key mechanism in preventing their aberrant expression and their hypomethylation is often associated with TEs reactivation due to various environmental stressors (Koturbash et al. 2011; Rudin and Thompson 2001). Therefore, expression of L1 ORF2 was measured, as it is critical for activation and retrotransposition of L1.

Compared with untreated controls, L1 ORF2 expression was 1.5 and 1.7 times higher after treatment with 0.5 and 30 μg/mL (administered doses), respectively; with a significant increase in expression at the higher dose (Figure 4B). Transcriptional activation of L1 ORF2 may result in retrotransposition on the "copy-paste" based mechanism, thus increasing the L1 copy numbers in the genome. Therefore, the L1 copy numbers were analyzed; however, no significant differences were identified (Figure 4C). Although not statistically significant, a 1.15- and 1.32-fold increase in the expression of *Alu* was observed after exposure to 0.5 and 30 μg/mL of PEPs, correspondingly (Figure 4B).

Effects of PEPs on DNA methyltransferases and methylcytosine dioxygenases expression

To investigate further the mechanisms of observed global and TEs-associated DNA hypomethylation, expression of DNA methyltransferases, key enzymes needed for establishment and maintenance of normal methylation patterns, was addressed. Compared with untreated cells,

a significant and dose-dependent reduction in the expression of all three DNA methyltransferases (*DNMT1, DNMT3A, DNMT3B*) was detected after PEPs exposure (Figure 4D). Additionally, expression of *UHRF1*, the protein that recruits *DNMT1* to the hemimethylated DNA sites, was significantly reduced after PEPs exposure in a dose-dependent manner. A significant and dose-dependent decreased expression of all three methylcytosine dioxygenases (*TET1-TET3*) was observed (Figure 4E).

Discussion

The study was aimed to evaluate the potential toxicity of varying doses of PEPs on human small airway epithelial cells (SAEC), macrophages (THP-1 cells) and lymphoblasts (TK6 cells). Using doses that approximate those associated with inhalation exposures, we measured cell membrane integrity, ROS production, inflammatory responses, DNA integrity and epigenetic changes. Since the aim of the study was to understand the biological response of cells following exposure to PEPs, administered doses on both the low end (0.5 μg/mL) and high end (100 μg/mL) of the spectrum were used. Low-end doses relate to exposure durations at consumer levels (*e.g.*, 8 hours of exposure to PEPs) while high-end doses relate to accumulated exposures of hundreds of hours of exposure. It must be noted that this dosimetric approach presented here may only be appropriate for short-term human exposures in the order of few days. Equating lifetime or multi-year exposure doses of accumulated PEPs mass in alveolar regions with bolus *in vitro* delivered doses ignores the differences in exposure dose and rate. These differences may span orders of magnitude, affecting clearance mechanisms; thus, leading to misleading results. Doses on the high-end of the spectrum should only be considered as the limit of an *in vitro* investigation and only when a wide range of doses, including low doses, is used

(Oberdorster et al. 2012). Therefore, the high administered dose of 100 μg/mL was included in order to get the full spectrum of dose-response relationships.

This publication is part of a series of companion papers evaluating the toxicological profile of PEPs. First, eleven commonly used printers were evaluated and ranked based on their PM emission profiles using our developed PEGS exposure platform (Pirela et al. 2014a). Secondly, the complete physicochemical and morphological properties of a number of toner powders and PEPs were thoroughly assessed (Pirela et al. 2014b). Thus, establishing that toner powders contain ENMs that become airborne during printing (consumer use). Thirdly, it was shown that low level exposures to PEPs ($PM_{0.1}$, $PM_{2.5}$) led to significant biological outcomes in an *in vitro* alveolar-capillary co-culture model (Sisler et al. 2014). Further investigation of paracrine signaling by epithelial and endothelial cells is of utmost significance, since cellular communication between these critical cell lines may play a major role in the pathogenesis of various pulmonary disorders.

Here, we investigated the toxicological potential of the smallest size fraction ($PM_{0.1}$) of PEPs from a laser printer emitting 1.26 particles/cm^3 (printer B1 in previous publications) using a mono-cell culture experimental design. Since the alveolar epithelium has direct contact with inhaled nanoparticles (Don Porto Carero et al. 2001) and the alveolar macrophages are the first responders to foreign particles in the lung, we exposed these cells to various concentrations of PEPs and observed the response to these particles. Results showed that both the epithelial cells (SAEC, at 100 μg/mL, delivered dose) and macrophages (THP-1 cells) (at 2.59 μg/mL, delivered dose) were negatively affected by treatment with PEPs and experienced >50% cell death. Of note, macrophages (THP-1 cells) seem to be particularly sensitive to exposure to PEPs,

which proved to be more toxic than a known pulmonary irritant (MS-WF). This is in agreement with a study by Khatri et al. (2013b), which showed subtle dose-response changes in viability of macrophages (THP-1 cells) and small airway epithelial cells (SAEC) following a 24-hour exposure to particles sampled from a photocopier center that have similar chemical composition to PEPs. As previously shown in a companion study, SAEC viability following exposure to PEPs ($PM_{0.1}$) was lower than that to PEPs ($PM_{2.5}$) at a delivered dose of 2.5 μg/mL, indicative of greater potency of PEPs ($PM_{0.1}$) (Sisler et al. 2014).

In summary, these results point to significant cytotoxicity, which could lead to defects in the normal functioning of these cells, particularly on macrophages since they primarily engulf foreign materials. Cytotoxicity by PEPs to macrophages could impair their clearance mechanism, remodel cellular cross talking, and influence innate immune responses. The levels of cytotoxicity observed in the tested cell lines at doses comparable to inhalation exposures ranging from 7.8 to 1500 hours, further intensifies recent concerns that PM emitted from laser printers can trigger a response in the distal alveolar region, where the majority of the inhaled particles will deposit. Perhaps the toxicity of the PEPs can be attributed to their complex chemical composition, which includes various nano-sized metals/metal oxides that have already been shown to produce detrimental effects on various *in vitro* and *in vivo* studies. Such toxicological outcomes include decreased cell viability, increased production of ROS and agglomeration of internalized particles due to exposure to various ENMs (*e.g.*, titania, silica, ceria, iron oxide, silver) (Cohen et al. 2014a; Demokritou et al. 2013a; L'Azou et al. 2008; Watson et al. 2014). In summary, the vulnerability of respiratory bronchioles and alveoli to exogenous materials highlights the necessity to understand the level of damage PEPs can have on consumers' respiratory system and other organ systems (*i.e.*, cardiovascular, immunological) without disregarding susceptible

individuals. It is also worth noting that similar to PEPs, our recent studies with photocopy center-sampled particles illustrate that those particles may produce adverse responses in the lung physiology of individuals exposed even at relatively low doses (Khatri et al. 2013a; Khatri et al. 2013b; Pirela et al. 2013; Pirela et al. 2014b).

Another relevant parameter used to evaluate adverse effects of exposures to airborne PM in general is secretion of cytokines. Expression of these chemical messengers in SAEC was evaluated here to quantify the inflammatory response to PEPs. Results showed that exposure to PEPs ($PM_{0.1}$) significantly up-regulated MCP-1, MIP-1b, PDGF-AA, IL-1RA, IL-6 and RANTES. These mediators are critical to the innate immune process, which recruits leukocytes to the site of injury/inflammation (Hayden et al. 2009; Ritter et al. 2005). An increase in IL-6 and MCP-1 was also observed in a companion paper following a low level exposure to PEPs ($PM_{0.1}$, $PM_{2.5}$) using an epithelial-endothelial cell co-culture system (Sisler et al. 2014). These results are in agreement with a study bySetyawati et al. (2013), in which endothelial cells treated with nano-titania reacted in a non-receptor-mediated mechanism and triggered endothelial cell leakiness. Similarly, macrophages, primary nasal and small airway epithelial cells exposed to various doses of photocopy center-sampled particles exhibited elevated secretion of various cytokines, namely GM-CSF, IL-1b, IL-6, IL-8, TNF-a and VEGF (Khatri et al. 2013b). Furthermore, these were also overexpressed in nasal lavage of human volunteers exposed to copy center particles for 6 hours (Khatri et al. 2013a). Particularly, MCP-1 is known to be a monocyte chemoattractant produced by monocytes and macrophages due to several stressors (*e.g.*, oxidative damage, cytokine, growth factors). This chemokine regulates migration and infiltration of monocytes, memory T cells and natural killer cells to the site of injury, mainly leading to a differentiation of a Th2 response. Therefore, a modification in the levels of MCP-1 may hint that exposure to PEPs

can affect monocyte/macrophage recruitment in the lung for phagocytosis of invading pathogens (Deshmane et al. 2009). Moreover, expression of MCP-1, can in turn contribute to an increase in the levels of IL-6, which blocks apoptosis. A study by Liu et al. (2007) found that MCP-1 mediated survival of fibroblasts by elevating IL-6 levels *via* the IL-6/STAT3 signaling pathway. Consequently, apoptosis of fibroblasts was inhibited resulting in continued lung fibrosis. Additionally, the RANTES chemokine has been found to be strongly upregulated due to asbestos exposure, which causes malignant mesothelioma (Comar et al. 2014). Other cytokines that were significantly affected in pleural fibrosis as well as in malignant mesotheliomas include IL-6, IL-1b and IL-8, possibly through inflammasome activation (Hillegass et al. 2013). These same cytokines were observed to be affected post-exposure to PEPs (Sisler et al. 2014). Comparable changes in expression of TNFa, IL-1a and b, IL-6, MCP-1 and PDGF-AA were observed in mice exposed to multi-walled carbon nanotubes (Dong et al. 2015). Thus, the authors concluded that such exposure was associated to an inflammatory and fibrotic response in the lung. However, more mechanistic studies looking at upstream effectors of the common process underlying the changes in cytokine expression, such as activation of NF-κB, are needed to enhance our understanding on inflammatory responses due to PEPs exposures. The authors plan to perform in-depth toxicological assessments to better understand the observed inflammatory responses and report findings in a future companion paper.

Aside from inflammatory responses, an increase in superoxide levels was evident in epithelial cells post-treatment with PEPs. Similar to our results, Sisler et al. (2014) observed an increment of ROS in endothelial cells after epithelial cells were exposed to low doses of PEPs using a co-culture platform. The same was not observed for the macrophages (THP-1 cells) treated with PEPs, whose cytotoxicity is almost 100% for the high dose of 100 μg/mL. However,

for the same dose, the cells produced low amounts of ROS suggesting the observed cytotoxicity might be mediated independently of ROS. Potential mechanisms may include direct activation of caspase-mediated apoptosis as observed by macrophages treated with zinc oxide nanoparticles (Wilhelmi et al. 2013), surface reactivity effects (Frohlich et al. 2009), or the HIF pathway (Nyga et al. 2015). More detailed mechanistic studies are needed in order to better understand the observed cytotoxicity. Overall, our data is consistent with studies showing an increase in extracellular levels of ROS and concomitant down-regulation of antioxidant levels following treatment with various doses of ENMs currently available in the market, such as ceria, titania and cobalt (Mittal and Pandey 2014; Wan et al. 2012; Zarogiannis et al. 2013).

Furthermore, the observed elevated levels of oxidation and inflammation prompted the assessment of DNA damage following exposure to PEPs using the newly developed high-throughput Nano-CometChip assay (Watson et al. 2014). The human lymphoblasts (TK6 cells) exposed to various doses of PEPs did not exhibit DNA damage, which is in disagreement with previous *in vitro* genotoxicity evaluations on human epithelial lung cells that displayed micronuclei formation and other characteristic injuries pertaining to DNA damage post-exposure to printer-emitted PM and toner powder (Gminski et al. 2011; Tang et al. 2012). Similar to our results, a study by Khatri et al. (2013b) using the comet assay concluded that treatment of macrophages with copy center sampled particles did not cause significant DNA damage. Lack of single-stranded DNA damage observed post-PEPs exposure could point to the possibility of double-stranded DNA damage or another mechanism responsible for the elevated cell death observed. It is important to note that heterogeneity in the PEPs chemical composition, well-documented in our earlier study (Pirela et al. 2014b), may explain differences in PEPs

genotoxicity. The issue of variability in chemical makeup of PEPs and genotoxicity deserves further research.

In this study, the ability of PEPs to affect the cellular epigenome was demonstrated. Specifically, preliminary evidence that short-term exposure to PEPs may result in altered DNA methylation in SAEC was found, thus affecting the methylation status of two of the most abundant TEs in the human genome – L1 and *Alu* that together comprise almost 30% of the genome. Moreover, in order to confirm these assumptions, future studies need to be performed.

DNA methylation is the key mechanism that prevents aberrant transcriptional activity of TEs (Smith et al. 2012). Loss of DNA methylation within the TEs often results in their transcriptional activation (Koturbash et al. 2011; Rudin and Thompson 2001). TEs reactivation, in turn, can result in retrotransposition and lead to genomic instability and development of diseases, including cancer. In this study, the expression of L1 ORF2 was found to be elevated, in a dose-dependent manner following exposure to both concentrations of PEPs. Similar trends, although not statistically significant, were also observed in *Alu* elements. This transcriptional activation, however, did not result in potential retrotransposition events since no significant increase in L1 copies number after exposure to PEPs was identified. It is possible that the time of exposure used in our study was not sufficient for detectable L1 retrotransposition. Indeed, a recent study on chemical exposure and L1 retrotransposition report L1 mobilization after 120 hours of exposure in cell culture (Terasaki et al. 2013). Further studies that will utilize longer exposures are clearly needed to determine the L1 retrotransposition abilities of PEPs.

A dose-dependent decrease in the expression of DNA methyltransferases caused by exposure to PEPs was detected in this study. These enzymes are essential for proper maintenance

of DNA methylation. Loss of DNA methyltransferases *in vitro* was previously reported after short-term exposure to PM (Miousse et al. 2014) and nano-SiO_2 particles (Gong et al. 2010), which were also associated with alterations in global and TEs DNA methylation. The observed down-regulation of DNA methyltransferases after exposure to PEPs may have detrimental effects on the levels of DNA methylation beyond the 24-hour time point used in this study. Importantly, we provide evidence that hypomethylation of TEs and loss of expression of DNA methyltransferases may occur after exposure to low, environmentally relevant doses (0.5 μg/mL) of PEPs. The mechanisms of such alterations may be associated with metals present in PEPs. In their vast majority, metals are weak mutagens, but can negatively affect the DNA methyltransferases enzymatic activity (Fragou et al. 2011). Furthermore, generation of ROS, associated with metals present in PEPs, may compromise the normal redox status, alter glutathione content and affect one-carbon metabolism pathways (Koturbash et al. 2012). Hypomethylation may be also mediated by decreased levels of *UHRF1* gene, which specifically interacts with DNA methyltransferases and hemimethylated sites on DNA (Ehrlich and Lacey 2013). The exact mechanisms of PEPs-associated epigenotoxicity, however, still need to be determined. The loss of TEs methylation was not associated with increased function of methylcytosine deoxygenases that navigate hydroxymethylation, the pathway involved in DNA demethylation (He et al. 2011; Ito et al. 2011). Further studies will be needed to delineate the exact effects of exposure to PEPs on the levels of 5-hmC and TET expression, especially with regards to studies indicating loss of 5-hmC TET in numerous diseases, including cancer (Jin et al. 2011; Li et al. 2011).

In summary, exposure to PEPs may have the potential to trigger an unfavorable biological response in several physiologically relevant cell lines. A rise in cell death, oxidative

stress, inflammation and altered methylation are some of the negative effects PEPs may have on the lung and may lead to increased risk of respiratory disorders in individuals who are exposed to emissions from laser printers.

Conclusion

The data indicate that PEPs emitted by laser printers can elicit unfavorable biological responses *in vitro*. Realistic exposures to PEPs led to significant changes in cell viability, hereditary genetic material changes, ROS and inflammatory mediators, among others. Moreover, the observed dysfunction of the DNA methylation and demethylation machinery associated with the loss of DNA methylation and reactivation of TEs, suggests that PEPs may cause a significant effect on the cellular epigenome. The results from such a comprehensive battery of toxicological assessments on PEPs are indicative of the cyto- and genotoxic potential of laser printer emissions at relevant doses comparable to current consumer and occupational settings. In order to further investigate the mechanism of toxicity in more detail, a study on the murine responses of exposures to PEPs *via* intratracheal instillation and whole-body inhalation is currently in progress. Taken together, our mechanistically oriented toxicological studies could reveal the biological interaction of PEPs following exposures comparable to those experienced by a consumer when using laser printers.

References

Anjilvel S, Asgharian B. 1995. A multiple-path model of particle deposition in the rat lung. Fundam Appl Toxicol 28:41–50.

Antonini J, Lawryk N, Murthy G, Brain J. 1999. Effect of welding fume solubility on lung macrophage viability and function in vitro. J Toxicol Environ Health A 58:343–363.

Antonini J, Zeidler-Erdely P, Young S, Roberts J, Erdely A. 2012. Systemic immune cell response in rats after pulmonary exposure to manganese-containing particles collected from welding aerosols. J Immunotoxicol 9:184–192.

Ayres FM, Cruz ADd, Steele P, Glickman BW. 2006. Low doses of gamma ionizing radiation increase HPRT mutant frequencies of TK6 cells without triggering the mutator phenotype pathway. Genetics and molecular biology 29:558–561.

Baccarelli A, Wright RO, Bollati V, Tarantini L, Litonjua AA, Suh HH, et al. 2009. Rapid DNA methylation changes after exposure to traffic particles. American journal of respiratory and critical care medicine 179:572–578.

Bai R, Zhang L, Liu Y, Meng L, Wang L, Wu Y, et al. 2010. Pulmonary responses to printer toner particles in mice after intratracheal instillation. Toxicol Lett 199:288–300.

Bajpayee M, Kumar A, Dhawan A. 2013. The comet assay: Assessment of in vitro and in vivo DNA damage. Methods in molecular biology 1044:325–345.

Campos AC, Molognoni F, Melo FH, Galdieri LC, Carneiro CR, D'Almeida V, et al. 2007. Oxidative stress modulates DNA methylation during melanocyte anchorage blockade associated with malignant transformation. Neoplasia 9:1111–1121.

Cohen J, Deloid G, Pyrgiotakis G, Demokritou P. 2013. Interactions of engineered nanomaterials in physiological media and implications for in vitro dosimetry. Nanotoxicology 7:417–431.

Cohen JM, Derk R, Wang L, Godleski J, Kobzik L, Brain J, et al. 2014a. Tracking translocation of industrially relevant engineered nanomaterials (ENMs) across alveolar epithelial monolayers in vitro. Nanotoxicology 8 Suppl 1:216–225.

Cohen JM, Teeguarden JG, Demokritou P. 2014b. An integrated approach for the in vitro dosimetry of engineered nanomaterials. Part Fibre Toxicol 11:20.

Daigneault M, Preston JA, Marriott HM, Whyte MK, Dockrell DH. 2010. The identification of markers of macrophage differentiation in pma-stimulated THP-1 cells and monocyte-derived macrophages. PloS one 5:e8668.

DeLoid G, Cohen JM, Darrah T, Derk R, Rojanasakul L, Pyrgiotakis G, et al. 2014. Estimating the effective density of engineered nanomaterials for in vitro dosimetry. Nature communications 5:3514.

Demokritou P, Kavouras IG, Ferguson ST, Koutrakis P. 2002. Development of a high volume cascade impactor for toxicological and chemical characterization studies. Aerosol Science and Technology 36:925–933.

Demokritou P, Buchel R, Molina RM, Deloid GM, Brain JD, Pratsinis SE. 2010. Development and characterization of a versatile engineered nanomaterial generation system (VENGES) suitable for toxicological studies. Inhal Toxicol 22 Suppl 2:107–116.

Demokritou P, Gass S, Pyrgiotakis G, Cohen JM, Goldsmith W, McKinney W, et al. 2013a. An in vivo and in vitro toxicological characterisation of realistic nanoscale ceo2 inhalation exposures. Nanotoxicology 7:1338–1350.

Deshmane SL, Kremlev S, Amini S, Sawaya BE. 2009. Monocyte chemoattractant protein-1 (MCP-1): An overview. Journal of interferon & cytokine research : the official journal of the International Society for Interferon and Cytokine Research 29:313–326.

Doak SH, Griffiths SM, Manshian B, Singh N, Williams PM, Brown AP, et al. 2009. Confounding experimental considerations in nanogenotoxicology. Mutagenesis 24:285–293.

Don Porto Carero A, Hoet PH, Verschaeve L, Schoeters G, Nemery B. 2001. Genotoxic effects of carbon black particles, diesel exhaust particles, and urban air particulates and their extracts on a human alveolar epithelial cell line (A549) and a human monocytic cell line (THP-1). Environ Mol Mutagen 37:155–163.

Dong J, Porter DW, Batteli LA, Wolfarth MG, Richardson DL, Ma Q. 2015. Pathologic and molecular profiling of rapid-onset fibrosis and inflammation induced by multi-walled carbon nanotubes. Arch Toxicol 89:621–633.

Ehrlich M, Lacey M. 2013. DNA hypomethylation and hemimethylation in cancer. Advances in experimental medicine and biology 754:31–56.

Fragou D, Fragou A, Kouidou S, Njau S, Kovatsi L. 2011. Epigenetic mechanisms in metal toxicity. Toxicology mechanisms and methods 21:343–352.

Frohlich E, Samberger C, Kueznik T, Absenger M, Roblegg E, Zimmer A, et al. 2009. Cytotoxicity of nanoparticles independent from oxidative stress. The Journal of toxicological sciences 34:363–375.

Furukawa Y, Aizawa Y, Okada M, Watanabe M, Niitsuya M, Kotani M. 2002. Negative effect of photocopier toner on alveolar macrophages determined by in vitro magnetometric evaluation. Industrial health 40:214–221.

Gminski R, Decker K, Heinz C, Seidel A, Konczol M, Goldenberg E, et al. 2011. Genotoxic effects of three selected black toner powders and their dimethyl sulfoxide extracts in cultured human epithelial A549 lung cells in vitro. Environ Mol Mutagen 52:296–309.

Gong C, Tao G, Yang L, Liu J, Liu Q, Zhuang Z. 2010. SiO(2) nanoparticles induce global genomic hypomethylation in hacat cells. Biochemical and biophysical research communications 397:397–400.

Hayden PJ, Bolmarcich J, Armento A, Jackson J, G.R. H, T.L. K, et al. 2009. Role of Toll-like receptor (TLR) activation in asthma exacerbation: Experiments with in vitro models of human airway epithelial cells (epiairway) and epithelial cell/fibroblast co-cultures (epiairway-ft). In: American Thoracic Society Annual Meeting. San Diego, CA.

He C, Morawska L, Taplin L. 2007. Particle emission characteristics of office printers. Environmental science & technology 41:6039–6045.

He YF, Li BZ, Li Z, Liu P, Wang Y, Tang Q, et al. 2011. Tet-mediated formation of 5-carboxylcytosine and its excision by TDG in mammalian DNA. Science 333:1303–1307.

Holder AL, Goth-Goldstein R, Lucas D, Koshland CP. 2012. Particle-induced artifacts in the MTT and LDH viability assays. Chemical research in toxicology 25:1885–1892.

International Data Corporation (IDC). 2014. Idc finds continued growth in the worldwide hardcopy peripherals market in the fourth quarter of 2013 Framingham, Massachusetts.

Ito S, Shen L, Dai Q, Wu SC, Collins LB, Swenberg JA, et al. 2011. TET proteins can convert 5-methylcytosine to 5-formylcytosine and 5-carboxylcytosine. Science 333:1300–1303.

Jin SG, Jiang Y, Qiu R, Rauch TA, Wang Y, Schackert G, et al. 2011. 5-hydroxymethylcytosine is strongly depleted in human cancers but its levels do not correlate with IDH1 mutations. Cancer research 71:7360–7365.

Jones PA. 2012. Functions of DNA methylation: Islands, start sites, gene bodies and beyond. Nature reviews Genetics 13:484–492.

Khatri M, Bello D, Gaines P, Martin J, Pal AK, Gore R, et al. 2013a. Nanoparticles from photocopiers induce oxidative stress and upper respiratory tract inflammation in healthy volunteers. Nanotoxicology 7:1014–1027.

Khatri M, Bello D, Pal AK, Cohen JM, Woskie S, Gassert T, et al. 2013b. Evaluation of cytotoxic, genotoxic and inflammatory responses of nanoparticles from photocopiers in three human cell lines. Part Fibre Toxicol 10:42.

Kimura A, Miyata A, Honma M. 2013. A combination of in vitro comet assay and micronucleus test using human lymphoblastoid TK6 cells. Mutagenesis 28:583–590.

Koturbash I, Scherhag A, Sorrentino J, Sexton K, Bodnar W, Tryndyak V, et al. 2011. Epigenetic alterations in liver of C57BL/6J mice after short-term inhalational exposure to 1,3-butadiene. Environmental health perspectives 119:635–640.

Koturbash I, Simpson NE, Beland FA, Pogribny IP. 2012. Alterations in histone H4 lysine 20 methylation: Implications for cancer detection and prevention. Antioxidants & redox signaling 17:365–374.

L'Azou B, Jorly J, On D, Sellier E, Moisan F, Fleury-Feith J, et al. 2008. In vitro effects of nanoparticles on renal cells. Part Fibre Toxicol 5:22.

Lacy P, Stow JL. 2011. Cytokine release from innate immune cells: Association with diverse membrane trafficking pathways. Blood 118:9–18.

Li Z, Cai X, Cai CL, Wang J, Zhang W, Petersen BE, et al. 2011. Deletion of TET2 in mice leads to dysregulated hematopoietic stem cells and subsequent development of myeloid malignancies. Blood 118:4509–4518.

Lu X, Miousse IR, Pirela SV, Melnyk S, Koturbash I, Demokritou P. 2015. Short-term exposure to engineered nanomaterials affects cellular epigenome. Nanotoxicology doi: 10.3109/17435390.2015.1025115

Madrigano J, Baccarelli A, Mittleman MA, Wright RO, Sparrow D, Vokonas PS, et al. 2011. Prolonged exposure to particulate pollution, genes associated with glutathione pathways, and DNA methylation in a cohort of older men. Environmental health perspectives 119:977–982.

Miousse IR, Chalbot MC, Aykin-Burns N, Wang X, Basnakian A, Kavouras IG, et al. 2014. Epigenetic alterations induced by ambient particulate matter in mouse macrophages. Environ Mol Mutagen 55:428–435.

Miousse IR, Shao L, Chang J, Feng W, Wang Y, Allen AR, Turner J, Stewart B, Raber J, Zhou D, Koturbash I. 2014. Exposure to low dose 56Fe irradiation induces long-term epigenetic alterations in mouse bone marrow hematopoietic progenitor and stem cells. Radiat Res 182:92–101.

Miousse IR, Chalbot MC, Lumen A, Ferguson A, Kavouras IG, Koturbash I. 2015. Response of transposable elements to elements to environmental stressors. Mutat Res Rev Mutat Res.

Mittal S, Pandey AK. 2014. Cerium oxide nanoparticles induced toxicity in human lung cells: Role of ROS mediated DNA damage and apoptosis. BioMed research international 2014:891–934.

Monteiro-Riviere NA, Inman AO, Zhang LW. 2009. Limitations and relative utility of screening assays to assess engineered nanoparticle toxicity in a human cell line. Toxicology and applied pharmacology 234:222–235.

Morawska L, He C, Johnson G, Jayaratne R, Salthammer T, Wang H, et al. 2009. An investigation into the characteristics and formation mechanisms of particles originating from the operation of laser printers. Environmental science & technology 43:1015–1022.

Morimoto Y, Oyabu T, Horie M, Kambara T, Izumi H, Kuroda E, et al. 2013. Pulmonary toxicity of printer toner following inhalation and intratracheal instillation. Inhal Toxicol 25:679–690.

Nyga A, Hart A, Tetley TD. 2015. Importance of the HIF pathway in cobalt nanoparticle-induced cytotoxicity and inflammation in human macrophages. Nanotoxicology 13:1–13.

O'Hagan HM, Wang W, Sen S, Destefano Shields C, Lee SS, Zhang YW, et al. 2011. Oxidative damage targets complexes containing DNA methyltransferases, SIRT1, and polycomb members to promoter CpG islands. Cancer cell 20:606–619.

Pal AK, Cohen J, Bello D, Demokritou P. 2014. Implications of in-vitro dosimetry on toxicological ranking of low aspect ratio engineered nanomaterials. Nanotoxicology 12:1-13.

Pirela S, Molina R, Watson C, Cohen JM, Bello D, Demokritou P, et al. 2013. Effects of copy center particles on the lungs: A toxicological characterization using a Balb/c mouse model. Inhal Toxicol 25:498–508.

Pirela SV, Pyrgiotakis G, Bello D, Thomas T, Castranova V, Demokritou P. 2014a. Development and characterization of an exposure platform suitable for physico-chemical, morphological and toxicological characterization of printer-emitted particles (PEPs). Inhal Toxicol 26:400–408.

Pirela SV, Sotiriou GA, Bello D, Shafer M, Bunker KL, Castranova V, et al. 2014b. Consumer exposures to laser printer-emitted engineered nanoparticles: A case study of life-cycle implications from nano-enabled products. Nanotoxicology:1–9.

Ritter M, Mennerich D, Weith A, Seither P. 2005. Characterization of Toll-like receptors in primary lung epithelial cells: Strong impact of the TLR3 ligand poly(i:C) on the regulation of Toll-like receptors, adaptor proteins and inflammatory response. J Inflamm (Lond) 2:16.

Rudin CM, Thompson CB. 2001. Transcriptional activation of short interspersed elements by DNA-damaging agents. Genes, chromosomes & cancer 30:64–71.

Setyawati MI, Tay CY, Chia SL, Goh SL, Fang W, Neo MJ, et al. 2013. Titanium dioxide nanomaterials cause endothelial cell leakiness by disrupting the homophilic interaction of VE-cadherin. Nature communications 4:1673.

Sisler JD, Pirela SV, Friend S, Farcas M, Schwegler-Berry D, Shvedova A, et al. 2014. Small airway epithelial cells exposure to printer-emitted engineered nanoparticles induces cellular effects on human microvascular endothelial cells in an alveolar-capillary co-culture model. Nanotoxicology:1–11.

Smith ZD, Chan MM, Mikkelsen TS, Gu H, Gnirke A, Regev A, et al. 2012. A unique regulatory phase of DNA methylation in the early mammalian embryo. Nature 484:339–344.

Sotiriou GA, Diaz E, Long MS, Godleski J, Brain J, Pratsinis SE, et al. 2012. A novel platform for pulmonary and cardiovascular toxicological characterization of inhaled engineered nanomaterials. Nanotoxicology 6:680–690.

Sriram K, Lin GX, Jefferson AM, Roberts JR, Andrews RN, Kashon ML, et al. 2012. Manganese accumulation in nail clippings as a biomarker of welding fume exposure and neurotoxicity. Toxicology 291:73–82.

Tang T, Gminski R, Konczol M, Modest C, Armbruster B, Mersch-Sundermann V. 2012. Investigations on cytotoxic and genotoxic effects of laser printer emissions in human epithelial A549 lung cells using an air/liquid exposure system. Environ Mol Mutagen 53:125–135.

Terasaki N, Goodier JL, Cheung LE, Wang YJ, Kajikawa M, Kazazian HH, Jr., et al. 2013. In vitro screening for compounds that enhance human l1 mobilization. PloS one 8:e74629.

Wan R, Mo Y, Feng L, Chien S, Tollerud DJ, Zhang Q. 2012. DNA damage caused by metal nanoparticles: Involvement of oxidative stress and activation of ATM. Chemical research in toxicology 25:1402–1411.

Wang H, He C, Morawska L, McGarry P, Johnson G. 2012. Ozone-initiated particle formation, particle aging, and precursors in a laser printer. Environmental science & technology 46:704–712.

Watson C, Ge J, Cohen J, Pyrgiotakis G, Engelward BP, Demokritou P. 2014. High-throughput screening platform for engineered nanoparticle-mediated genotoxicity using CometChip technology. ACS nano 8:2118–2133.

Wilhelmi V, Fischer U, Weighardt H, Schulze-Osthoff K, Nickel C, Stahlmecke B, et al. 2013. Zinc oxide nanoparticles induce necrosis and apoptosis in macrophages in a p47phox- and Nrf2-independent manner. PloS one 8:e65704.

Zarogiannis SG, Filippidis AS, Fernandez S, Jurkuvenaite A, Ambalavanan N, Stanishevsky A, et al. 2013. Nano-TiO(2) particles impair adhesion of airway epithelial cells to fibronectin. Respiratory physiology & neurobiology 185:454–460.

Zeidler-Erdely P, Battelli L, Salmen-Muniz R, Li Z, Erdely A, Kashon M, et al. 2011. Lung tumor production and tissue metal distribution after exposure to manual metal arc-stainless steel welding fume in A/J and C57BL/6J mice. J Toxicol Environ Health A 74:728–736.

Table 1. Properties of laser printer emitted particle dispersions.

Material	Media	d_H (nm)	PdI	ζ (mV)	σ (mS/cm)	ρ_{agg} (g/cm^3)
PEPs ($PM_{0.1}$)	DI H_2O	178.3 ± 3.459	0.403 ± 0.050	-20.6 ± 1.87	0.185 ± $5.8x10^{-4}$	-
	RPMI/ 10%HS	272.5 ± 22.27	0.688 ± 0.178	-9.80 ± 1.31	3.61 ± 0.246	1.19
	RPMI/ 10% FBS	227.3 ± 105.0	0.485 ± 0.247	9.55 ± 2.89	7.01 ± 0.960	1.56
	SAGM	381.7 ± 40.23	0.586 ± 0.048	9.97 ± 2.77	2.52 ± 0.0721	2.39
Mild steel welding fumes (MS-WF)	DI H_2O	2197 ± 118.4	0.561 ± 0.325	8.52 ± 1.24	0.028 ± $0.93x10^{-4}$	-
	RPMI/ 10%HS	1878.3 ± 395.89	0.236 ± 0.080	10.5 ± 0.757	11.9 ± 0.289	1.48
	RPMI/ 10% FBS	1502 ± 96.26	0.236 ± 0.080	12.1 ± 2.66	11.5 ± 1.10	1.56
	SAGM	1526.7 ± 259.63	0.198 ± 0.041	18.8 ± 0.9	10.5 ± 0.462	1.37
SiO_2	DI H_2O	142.5 ± 2.364	0.207 ± 0.013	33.6 ± 1.70	0.008 ± $4.4x10^{-5}$	-
	RPMI/ 10%HS	173.4 ± 13.36	0.541 ± 0.027	11.4 ± 3.60	11.2 ± 0.874	1.3
	RPMI/ 10% FBS	114.6 ± 0.100	0.324 ± 0.009	9.33 ± 0.841	11.6 ± 0.833	1.2
	SAGM	207.7 ± 6.029	0.583 ± 0.078	12.7 ± 1.39	11.1 ± 0.436	1.12

Notes: Values represent the mean (± SD) of a triplicate reading. '-' data not available. d_H: hydrodynamic diameter, PdI: polydispersity index, ζ: zeta potential, σ: specific conductance, ρ_{agg}: effective density, DI H_2O: deionized water, RPMI: Roswell Park Memorial Institute medium, HS: horse serum, FBS: fetal bovine serum, SAGM: small airway epithelial cell growth medium.

Table 2. *In vitro* doses and the respective consumer inhalation exposure duration to PEPs.

Cell administered dose[a] (µg/mL)	**Cell delivered dose[a] (µg/mL) SAEC**	**Corresponding consumer inhalation exposure duration (hours) to PEPs [b] SAEC**	**Cell delivered dose[a] (µg/mL) THP-1**	**Corresponding consumer inhalation exposure duration (hours) to PEPs [b] THP-1**
0.5	0.5	15.0	0.26	7.8
5	5	75.2	2.6	39.0
10	10	150.4	5.2	77.9
20	20	300.7	10.4	155.8
30	30	451.1	15.6	233.7
40	40	601.4	20.8	311.5
100	100	1503.6	52.0	778.9

Notes:

[a] *In vitro* administered- and delivered doses are based on a 24-hour *in vitro* exposure.

[b] Calculations of the corresponding consumer inhalation exposure duration (hours) to PEPs was based on the added values of deposition mass flux (µg/m^2•min) in the various human airways, excluding head airways: the conducting zone (generations 0 to 16) and the transitional and respiratory zones (generations 17 through 23).

Figure Legends

Figure 1. Percent cytotoxicity of cells determined using LDH assay following exposure to PEPs ($PM_{0.1}$), SiO_2 and MS-WF on three human cell lines. All values are represented as mean ± SE. Values significantly different from the [*] untreated, [a] PEPs ($PM_{0.1}$) dose-matched, [b] PEPs ($PM_{0.1}$) 100 µg/mL, [c] SiO_2 100 µg/mL, [d] MS-WF 5 µg/mL treatment groups. Bar represents a significant difference in measurements across the treatment groups with a p level < 0.05.

Figure 2. Percentage increase of reactive oxygen species compared to untreated control cells measured in supernatant from SAEC and THP-1 following a 24-hour exposure to PEPs ($PM_{0.1}$), SiO_2 and MS-WF. All values are represented as mean ± SE. [a] Significantly different from PEPs ($PM_{0.1}$), dose-matched treatment group. Bar represents a significant difference in measurements across the treatment groups with a p level < 0.05.

Figure 3. Measured levels of cytokines and chemokines in supernatant of SAEC exposed to PEPs, SiO_2 and MS-WF for 24 hours. All values are represented as mean ± SE. Bar represents a significant difference in measurements across the treatment groups with a p level < 0.05.

Figure 4. DNA methylation observed in SAEC exposed to PEPs for 24 hours as measured relative to the untreated control. (A) fold change in 5-meC in TEs (B) mRNA expression of TEs (C) copy number (D) gene expression of *DNMTs* and accessory protein *UHRF1*. (E) Expression of methylcytosine dioxygenases (*TET1-TET3*) in SAEC exposed to PEPs for 24 hours. All values are represented as mean ± SE.* p level < 0.05, ** p level < 0.01, *** p level < 0.001.

Figure 1.

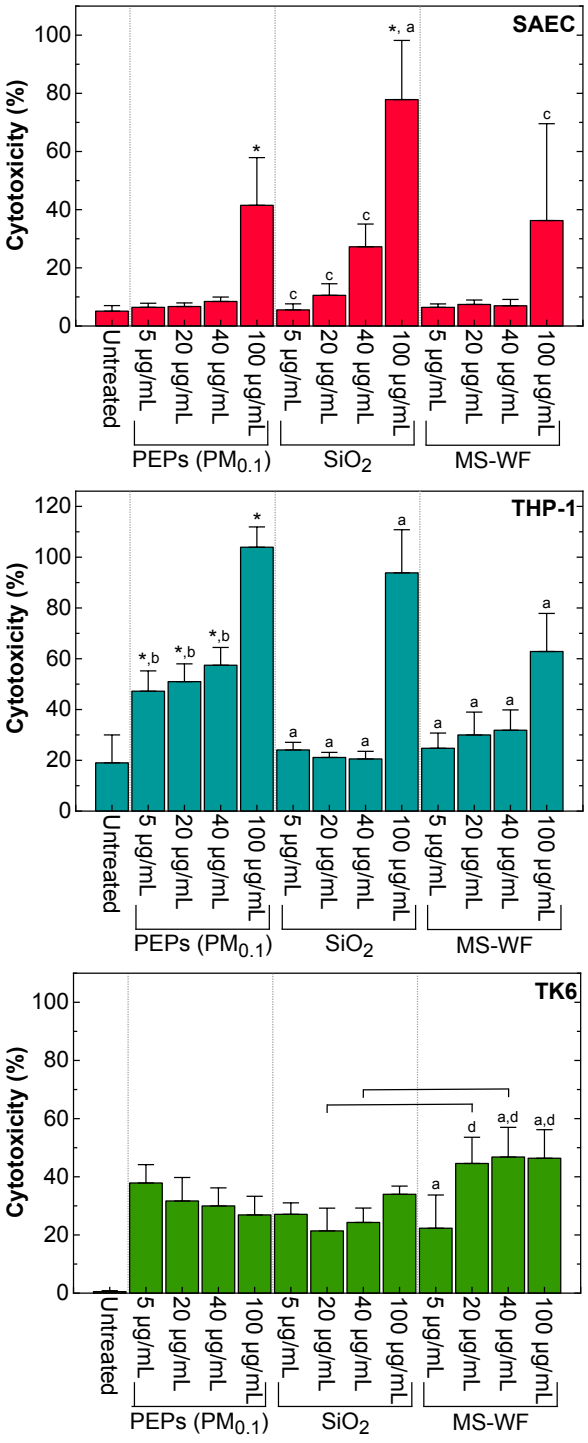
SAEC
THP-1
TK6
Cytotoxicity (%)
Untreated
5 μg/mL
20 μg/mL
40 μg/mL
100 μg/mL
PEPs (PM0.1)
SiO2
MS-WF

Figure 2.

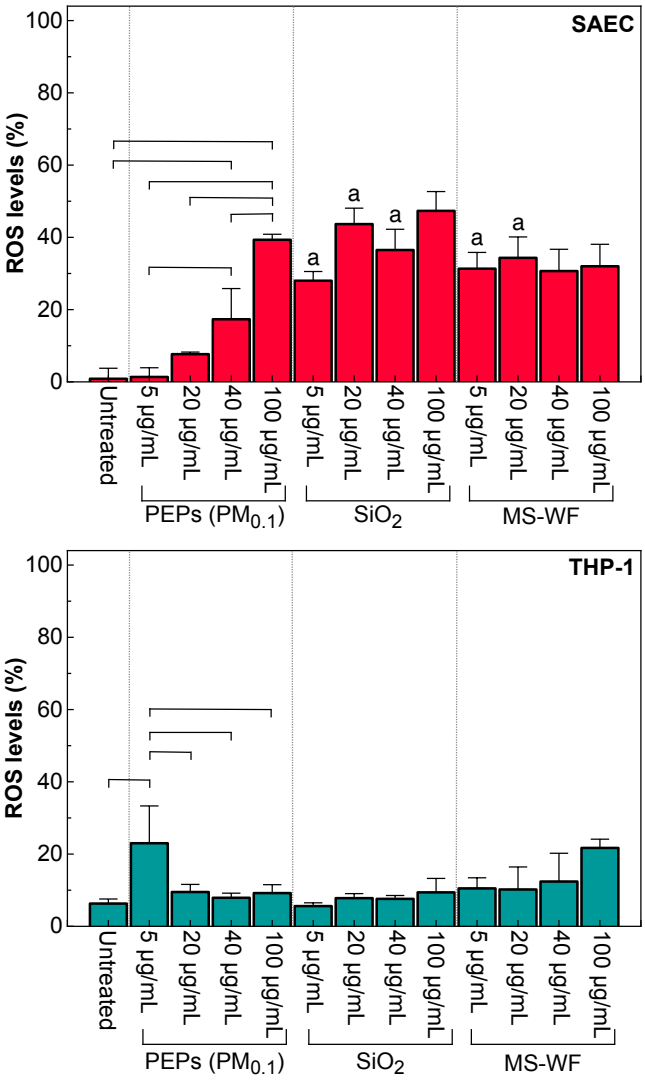
SAEC
THP-1
ROS levels (%)
0
20
40
60
80
100
a
Untreated
5 μg/mL
20 μg/mL
40 μg/mL
100 μg/mL
PEPs (PM0.1)
SiO2
MS-WF

Figure 3.

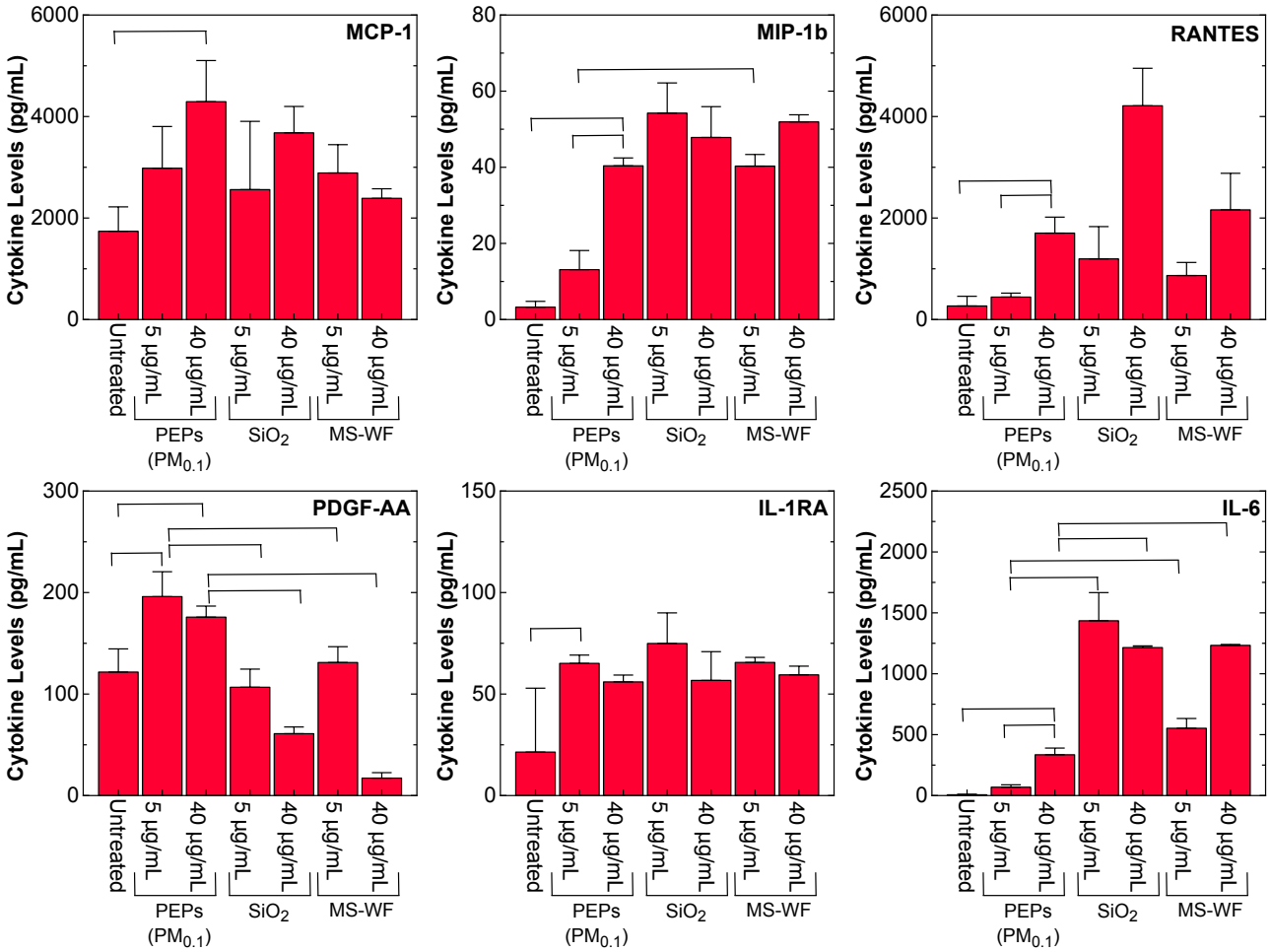
MCP-1
MIP-1b
RANTES
PDGF-AA
IL-1RA
IL-6
Cytokine Levels (pg/mL)
Untreated
5 μg/mL
40 μg/mL
PEPs
(PM0.1)
SiO2
MS-WF

Figure 4.

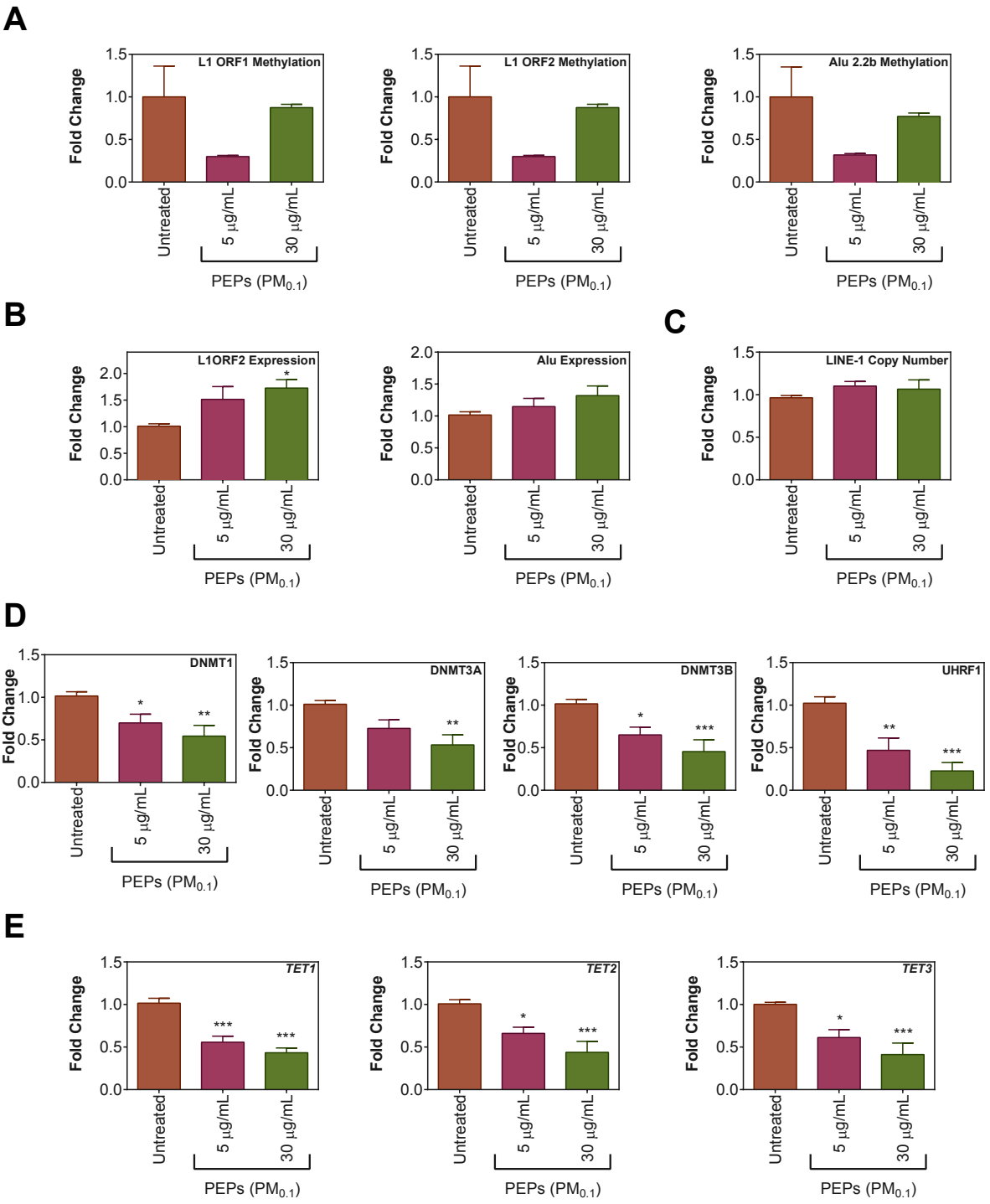
A
L1 ORF1 Methylation
L1 ORF2 Methylation
Alu 2.2b Methylation
B
L1ORF2 Expression
Alu Expression
C
LINE-1 Copy Number
D
DNMT1
DNMT3A
DNMT3B
UHRF1
E
TET1
TET2
TET3
Fold Change
Untreated
5 µg/mL
30 µg/mL
PEPs (PM0.1)